© 2015. Published by The Company of Biologists Ltd | Journal of Cell Science (2015) 128, 923–934 doi:10.1242/jcs.158998

RESEARCH ARTICLE

SEPT12 orchestrates the formation of mammalian sperm annulus by organizing core octameric complexes with other SEPT proteins

Yung-Che Kuo[1,2,*], Yi-Ru Shen[3,*], Hau-Inh Chen[4,5], Ying-Hung Lin[6], Ya-Yun Wang[3], Yet-Ran Chen[7], Chia-Yih Wang[2,8] and Pao-Lin Kuo[2,3,4,‡]

ABSTRACT

Male infertility has become a worldwide health problem, but the etiologies of most cases are still unknown. SEPT12, a GTP-binding protein, is involved in male fertility. Two SEPT12 mutations ($SEPT12^{T89M}$ and $SEPT12^{D197N}$) have been identified in infertile men who have a defective sperm annulus with a bent tail. The function of SEPT12 in the sperm annulus is still unclear. Here, we found that SEPT12 formed a filamentous structure with SEPT7, SEPT 6, SEPT2 and SEPT4 at the sperm annulus. The SEPT12-based septin core complex was assembled as octameric filaments comprising the SEPT proteins 12-7-6-2-2-6-7-12 or 12-7-6-4-4-6-7-12. In addition, the GTP-binding domain of SEPT12 was crucial for its interaction with SEPT7, and the N- and C-termini of SEPT12 were required for the interaction of SEPT12 with itself to polymerize octamers into filaments. Mutant mice carrying the $SEPT12^{D197N}$ mutation, which disrupts SEPT12 filament formation, showed a disorganized sperm annulus, bent tail, reduced motility and loss of the SEPT ring structure at the sperm annulus. These phenotypes were also observed in an infertile man carrying $SEPT12^{D197N}$. Taken together, our results demonstrate the molecular architecture of SEPT12 filaments at the sperm annulus, their mechanical support of sperm motility, and their correlation with male infertility.

KEY WORDS: SEPT12, Septin octamer, Sperm annulus, Spermiogenesis

INTRODUCTION

Approximately 10–15% of couples worldwide are affected by reduced fertility, and in roughly half of these cases the defects can be traced to the men (WHO, 1999; Jarow et al., 2002). A large proportion of infertile men have defects in the process of spermatogenesis (spermatogenetic defects). Although many pathways involved in this process have been elucidated in the past decade, the etiologies of most cases of male infertility remain unclear.

SEPT12, a GTP-binding protein with GTPase activity, has been implicated in sperm morphogenesis and male infertility. Mouse *Sept12* (Mm.87382) expression is restricted to spermatogenic cells (Hong et al., 2005; Lin et al., 2009). $Sept12^{+/-}$ chimeric mice (generated by gene targeting) are sterile with various sperm defects, including a bent tail and maturation arrest at the round spermatid stage (Lin et al., 2009). In addition, two SEPT12 mutations ($SEPT12^{T89M}$ and $SEPT12^{D197N}$) and one sequence variant (c.474G>A) have been identified in infertile men with distinctive sperm pathology, such as a defective annulus with a bent tail (Kuo et al., 2012; Lin et al., 2012). The two missense mutations are located within the GTP-binding domain of SEPT12. A consensus GTP-binding domain exists in all septins, and this promotes GTP binding and hydrolysis (Weirich et al., 2008). The two missense mutations abolish GTP hydrolytic activity, interfere with GTP binding, and profoundly perturb SEPT12 filament formation, resulting in male infertility. Thus, the SEPT12 filament is indispensable for reproduction. However, its composition in sperm is still unknown.

SEPT12 belongs to the septin family, which is a new type of cytoskeletal filament with conserved GTPase activity. Septins self-assemble into a core hexamer or octamer, which further elongates to form filaments or rings, thereby regulating various biological processes, for example, by serving as a membrane diffusion barrier or scaffold, or to alter membranous curvature (Mostowy and Cossart, 2012). Thirteen functional septin genes (*SEPT1* to *SEPT12* and *SEPT14*; *SEPT13* is a pseudogene) have been identified in humans. Based on sequence similarity, these septins are sub-divided into the following four subgroups: the SEPT2 subgroup (including SEPT1, SEPT2, SEPT4 and SEPT5), the SEPT3 subgroup (SEPT3, SEPT9 and SEPT12), the SEPT6 subgroup (SEPT6, SEPT8, SEPT10, SEPT11 and SEPT14), and the SEPT7 subgroup (SEPT7) (Kinoshita, 2003). It has been shown that the septin core hexameric complex contains members of the SEPT2, SEPT6 and SEPT7 subgroups, whereas octamers also include SEPT3 subgroup members (Sellin et al., 2011; Sellin et al., 2014). Septins in the same septin family subgroup can act as substitutes for one another at the same position of the core complex (Kinoshita, 2003; Sellin et al., 2011).

Crystallographic analysis of the mammalian septin core complex containing SEPT2, SEPT6 and SEPT7 has demonstrated that this complex is composed of elongated hexamers arranged in the order SEPT7–SEPT6–SEPT2–SEPT2–SEPT6–SEPT7 (Sirajuddin et al., 2007). Thus, the septin core complex is composed of a linear hetero-oligomer with mirroring symmetry, and it polymerizes into filaments with end-to-end associations. The interacting domains

[1]Department of Biochemistry and Molecular Cell Biology, School of Medicine, College of Medicine, Taipei Medical University, Taipei 11031, Taiwan. [2]Graduate Institute of Basic Medical Sciences, College of Medicine, National Cheng Kung University, Tainan 70403, Taiwan. [3]Department of Obstetrics and Gynecology, College of Medicine, National Cheng Kung University, Tainan 70403, Taiwan. [4]Department of Biochemistry and Molecular Biology, College of Medicine, National Cheng Kung University, Tainan 70403, Taiwan. [5]Department of Research, Taipei Tzu Chi Hospital, Buddhist Tzu Chi Medical Foundation, New Taipei City 23142, Taiwan. [6]Graduate Institute of Basic Medicine, College of Medicine, Fu Jen Catholic University, New Taipei City 24205, Taiwan. [7]Agricultural Biotechnology Research Center, Academia Sinica, Taipei 11529, Taiwan. [8]Department of Cell Biology and Anatomy, College of Medicine, National Cheng Kung University, Tainan 70403, Taiwan.
*These authors contributed equally to this work

‡Author for correspondence (paolink@mail.ncku.edu.tw)

Received 29 June 2014; Accepted 6 January 2015

Journal of Cell Science

Journal of Cell Science (2015) 128, 923–934 doi:10.1242/jcs.158998

of these septins have also been identified. The subunits interact with each other through alternating G- and NC-interfaces. The G-interfaces comprise the GTP-binding domains, whereas the NC-interfaces involve both the N- and C-terminal domains. The guanine-nucleotide-binding capacity of septins is vital for septin–septin interactions, filamentous organization and ring formation. Thus, the guanine nucleotide binding of septins is important to ensure structural integrity (Versele and Thorner, 2004; Nagaraj et al., 2008; Sirajuddin et al., 2009).

In the present study, we found that SEPT12 formed an octametric filament with SEPT7, 6, and 2 in the order 12-7-6-2-2-6-7-12 and that SEPT4 occupied the same position as SEPT2 to organize a 12-7-6-4-4-6-7-12 filament at the sperm annulus. Defects in GTP binding and the GTP hydrolytic activity of SEPT12 (*SEPT12*^{D197N} and *SEPT12*^{T89M}) interfered with the SEPT12–SEPT7 interaction and dissociated SEPT12 from the SEPT7–SEPT6–SEPT2 complex. A loss-of-function mutation of SEPT12 (SEPT12^{D197N}) in an infertile man was shown to result in a disorganized annulus and bent sperm tail due to disrupted SEPT12 filament formation. In addition, the sperm of SEPT12$^{D197N/D197N}$ mutant mice had a defective annulus, bent tail and reduced motility. Thus, the 12-7-6-2 or 12-7-6-4 SEPT filament maintains the structure of the sperm annulus and supports the mechanical integrity of sperm for proper maturation.

RESULTS

SEPT12 colocalizes with SEPT7, SEPT6, SEPT2 and SEPT4 in the sperm annulus

The sperm annulus is a submembrane SEPT ring structure demarcating the midpiece and the principle piece of the sperm tail (supplementary material Fig. S1A). To date, the best description of the complex of mammalian SEPT2, SEPT6 and SEPT7, which belong to the SEPT2, SEPT6 and SEPT7 subgroups, respectively, includes the formation of an elongated hexamer in the order SEPT7–SEPT6–SEPT2–SEPT2–SEPT6–SEPT7, as shown by crystallographic analysis (Sirajuddin et al., 2007). SEPT12, which belongs to the SEPT3 subgroup, is believed to assemble into octamers with SEPT7, SEPT6 and SEPT2 subgroup members and then to elongate to form longer filaments. To investigate the SEPT12 filament at the sperm annulus, we examined the protein localization of SEPT12 with SEPT7, SEPT6 and SEPT2 in normal subjects (healthy humans). Immunofluorescence staining of the sperm of a control subject showed strong SEPT12 signals at the sperm annulus, which is located at the distal end of the mitochondria (supplementary material Fig. S1B). The signals of SEPT7, SEPT6 and SEPT2, similar to SEPT12, were observed at the sperm annulus, indicating that SEPT12, SEPT7, SEPT6 and SEPT2 are annulus components. Indeed, double-staining with two antibodies showed that SEPT12 colocalized with SEPT7, SEPT6 and SEPT2 (Fig. 1A–C, insets). Thus, SEPT12, SEPT7, SEPT6 and SEPT2 colocalized in the sperm annulus of normal subjects, suggesting that SEPT12 can form a filamentous complex with SEPT7, SEPT6 and SEPT2 in the sperm annulus. SEPT4, which belongs to the SEPT2 subgroup, is a well-known component of the sperm annulus (Ihara et al., 2005; Kissel et al., 2005). We further investigated whether SEPT4 has a role in the SEPT12-associated filament at the sperm annulus. Immunostaining revealed that SEPT4 was located at the sperm annulus (supplementary material Fig. S1B) and colocalized with SEPT12 (Fig. 1D, insets), suggesting that SEPT4 also forms a complex with SEPT12 in the sperm annulus.

SEPT12 forms an octametric filament with SEPT7, SEPT6 and SEPT2 or SEPT4 in the order SEPT 12-7-6-2 or 12-7-6-4

We next examined whether SEPT12 interacted with SEPT7, SEPT6, SEPT2 and SEPT4. NT2/D1 cells from a human testicular embryonic carcinoma cell line were co-transfected with different septin-expressing constructs and cell extracts were analyzed by immunoprecipitation. SEPT7, SEPT6, SEPT2 and SEPT4 could be detected when SEPT12 was immunoprecipitated (Fig. 2A) and vice versa (Fig. 2B). These data imply that SEPT12 forms complexes with SEPT7, SEPT6, SEPT2 and SEPT4 in NT2/D1 cells. We further assessed the expression pattern of SEPT12 by immunostaining. Ectopic expression of SEPT12 led to the formation of a filamentous structure, as previously shown (Ding et al., 2007; Steels et al., 2007; Ding et al., 2008). SEPT7,

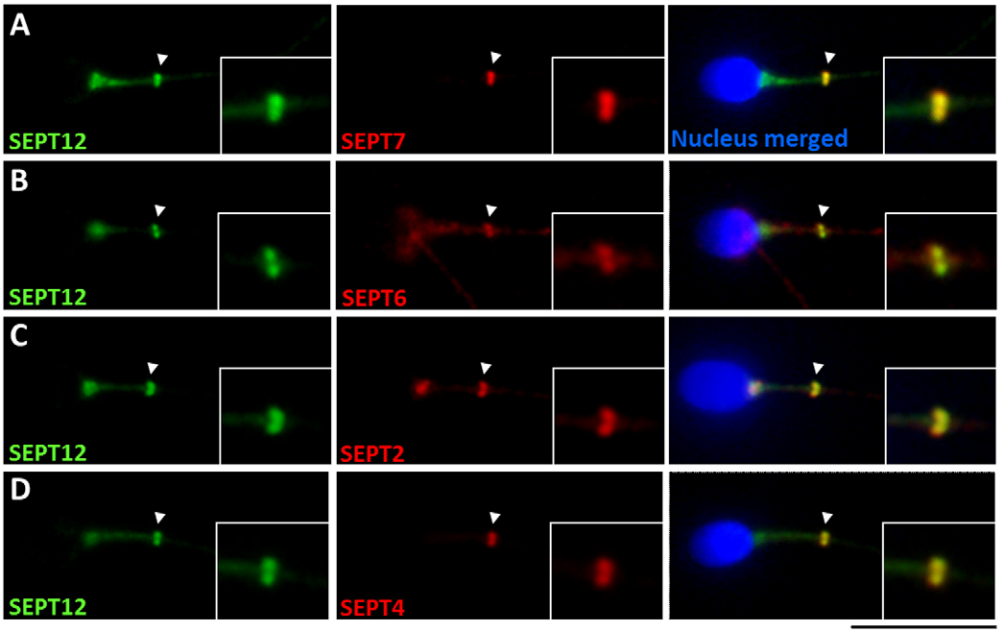

Fig. 1. SEPT12, SEPT7, SEPT6, SEPT2 and SEPT4 are components of sperm annulus. Immunofluorescence staining of normal sperm in a human fertile control showed signals for SEPT12 (A–D, green), SEPT7, SEPT6, SEPT2 and SEPT4 (A–D, red) at the annulus. Also shown are merged fluorescence staining images with additional staining of the sperm nuclei. Insets, magnified images of the annulus denoted by the arrowheads. Scale bar: 10 μm.

Journal of Cell Science (2015) 128, 923–934 doi:10.1242/jcs.158998

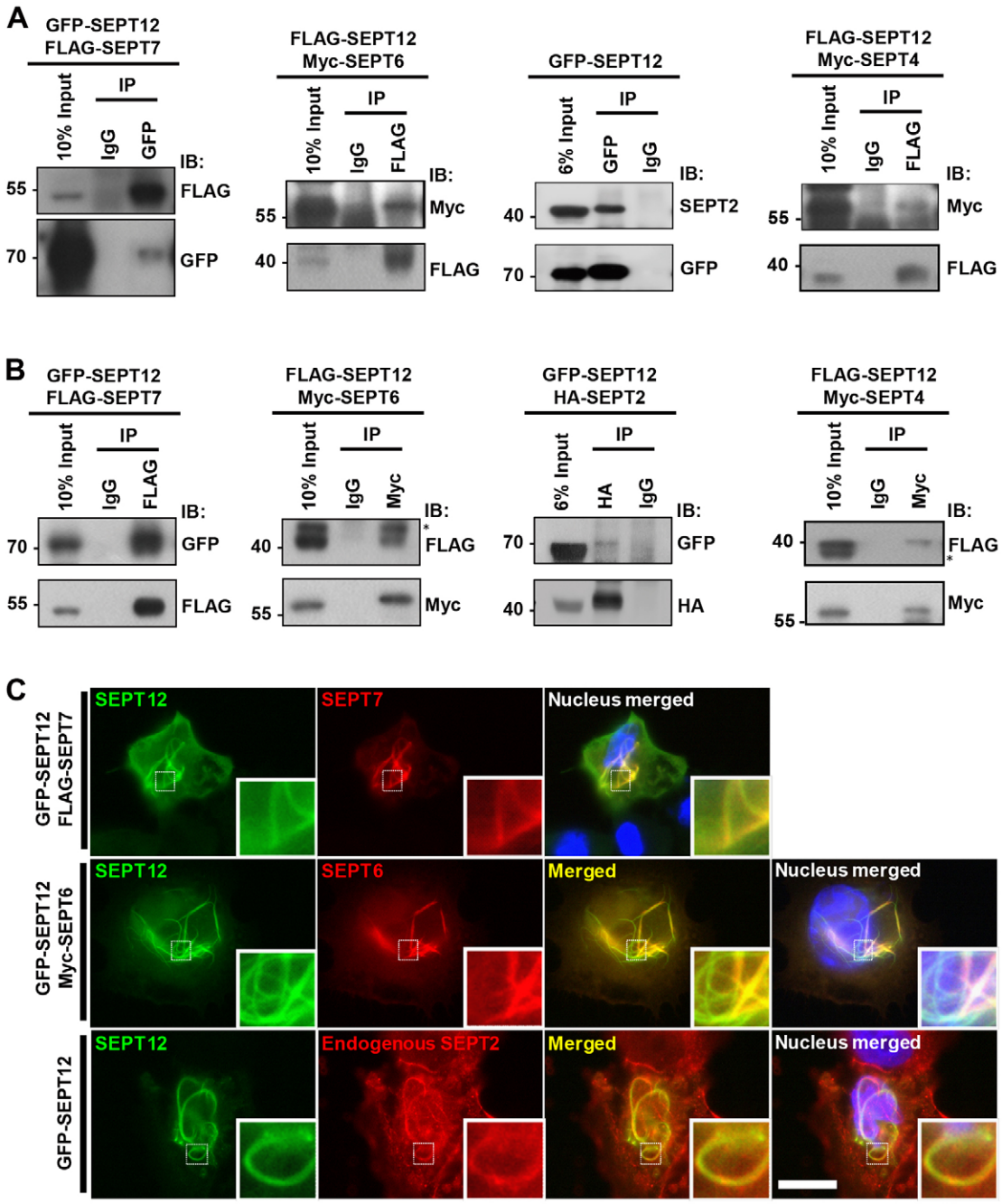

Fig. 2. SEPT12 associates with SEPT7, SEPT6 and SEPT2 or SEPT4 to form filaments. (A) Co-immunoprecipitation (IP) of EGFP–SEPT12 with FLAG–SEPT7 or endogenous SEPT2 and of FLAG–SEPT12 with Myc–SEPT6 or HA–SEPT4. NT2/D1 cells were co-transfected with various plasmids, as shown at the top. Lysates from transiently transfected cells were immunoprecipitated with an anti-FLAG, anti-Myc, anti-HA or anti-GFP antibody. IgG served as a negative control. Immunoblotting (IB) was carried out with the indicated antibodies shown on the right. A lane showing 10% of the input is also present. (B) Each septin–septin interaction was confirmed by reciprocal immunoprecipitation, except for EGFP–SEPT12, which was immunoprecipitated with HA–SEPT2. The asterisk represents a nonspecific band. (C) Formation of septin filaments in NT2/D1 cells. NT2/D1 cells were co-transfected with various plasmids, as shown on the left. Representative images from the immunofluorescence staining showing the subcellular patterns of GFP–SEPT12, FLAG–SEPT7, Myc–SEPT6 and endogenous SEPT2. The boxed areas showing filament fibers are magnified in the insets. Scale bar: 10 μm.

SEPT6 and SEPT2 were colocalized with filamentous SEPT12 (Fig. 2C). Thus, SEPT12 interacts with SEPT7, SEPT6 and SEPT2 and forms cytoplasmic filaments in NT2/D1 cells.

We further examined the assembly order of SEPT2, SEPT6, SEPT7 and SEPT12 within the SEPT12 complex. Different septins were co-expressed in 293T cells, and GFP–SEPT12 was used as a bait to capture SEPT2, SEPT6 and SEPT7. Following the transfection of all four septin plasmids, SEPT2, SEPT6 and SEPT7 were co-precipitated with GFP–SEPT12 (Fig. 3A, line 1) but not with GFP (Fig. 3A, line 5), demonstrating the specificity of the immunoprecipitation assay. In the absence of SEPT2 overexpression, SEPT12 still associated with SEPT6 or SEPT7, suggesting that the interaction between SEPT12, SEPT6 and SEPT7 is independent of SEPT2 (Fig. 3A, line 2; Fig. 3C).

Journal of Cell Science (2015) 128, 923–934 doi:10.1242/jcs.158998

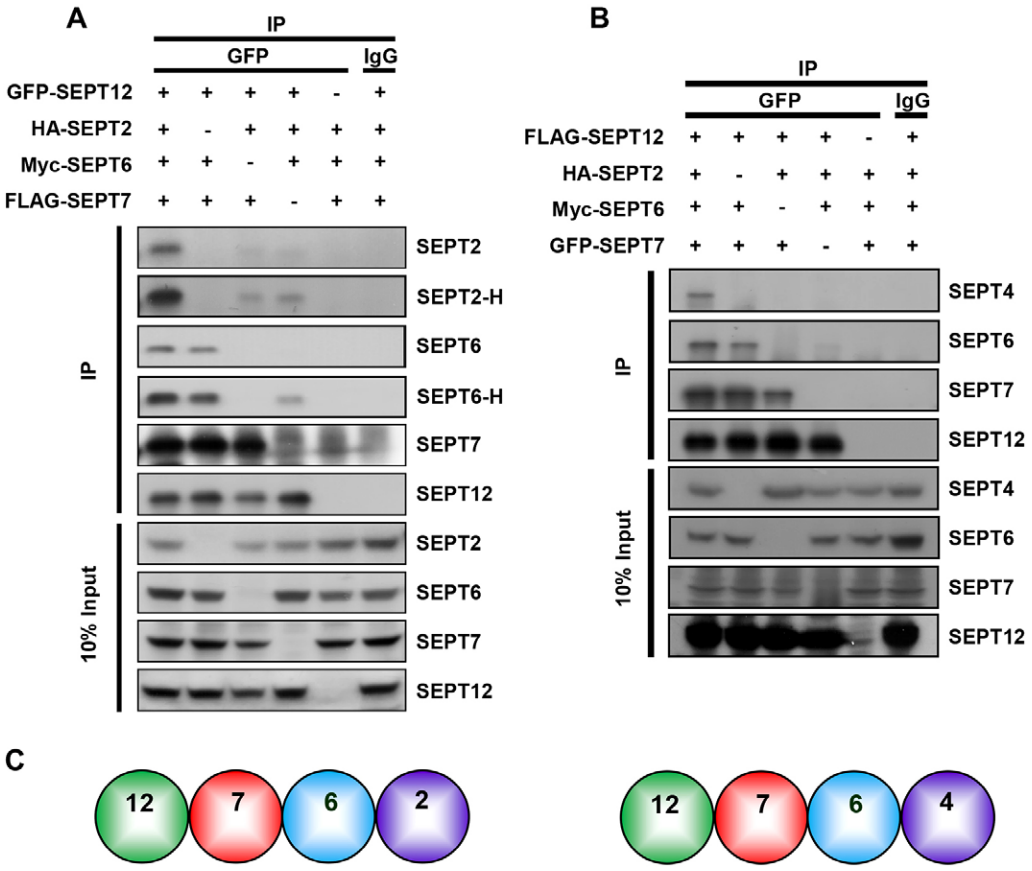

Fig. 3. SEPT12 complexes assemble in the orders SEPT12–SEPT7–SEPT6–SEPT2 and SEPT12–SEPT7–SEPT6–SEPT4. (A) GFP–SEPT12, HA–SEPT2, Myc–SEPT6 and FLAG–SEPT7 were transfected into 293T cells as indicated, and lysates were immunoprecipitated (IP) with an anti-GFP antibody. IgG served as a negative control. The expression levels of SEPT2, SEPT6, SEPT7 and SEPT12 were measured using anti-HA, anti-Myc, anti-FLAG, or anti-GFP antibody, respectively. -H, high-exposure film. Lanes showing 10% of the input are also present. (B) FLAG–SEPT12, HA–SEPT4, Myc–SEPT6 and GFP–SEPT7 were transfected into 293T cells, and lysates were immunoprecipitated with anti-FLAG antibody. The expression levels of SEPT4, SEPT6, SEPT7 and SEPT12 were measured using anti-HA, anti-Myc, anti-GFP or anti-FLAG antibody, respectively. (C) Schematic diagrams of the SEPT 12-7-6-2 and 12-7-6-4 complexes.

Without SEPT6 overexpression, the interaction between SEPT12 and SEPT2, but not SEPT7, was dramatically reduced (Fig. 3A, line 3), indicating that SEPT6 is required for the interaction between SEPT12 and SEPT2 but disposable for that between SEPT12 and SEPT7 (Fig. 3C). Without SEPT7 overexpression, the interactions between SEPT12 and SEPT2 as well as SEPT6 were dramatically reduced (Fig. 3A, line 4), indicating that SEPT12 interacts with SEPT6–SEPT2 through SEPT7. These results suggest the SEPT12-containing core complex is structured in the order SEPT12–SEPT7–SEPT6–SEPT2 (Fig. 3C). We also observed weak signals in the absence of overexpressed SEPT6 and/or SEPT7 using high-exposure film (Fig. 3A, SEPT2-H and SEPT6-H panels), suggesting that SEPT12 associated with these septins through endogenous septins.

Septins in the same subgroup are often interchangeable at same position of the oligomeric complex (Kinoshita, 2003; Sellin et al., 2011). We examined whether SEPT4 occupies the same position as SEPT2 in the SEPT12-organized complex. SEPT4 showed a similar interacting pattern to that of SEPT2 (Fig. 3B). These data indicate that SEPT4 holds same position as SEPT2 in this complex (Fig. 3C).

SEPT12 interacts with SEPT7–SEPT6–SEPT2 complex through its GTP-binding domain

Because the SEPT12–SEPT7 interaction is crucial for core complex assembly, we further examined the interacting domains by using truncated constructs of SEPT12 and SEPT7 in immunoprecipitation assays (supplementary material Fig. S2). The results showed that the GTP-binding domain (GBD) of SEPT12 interacted with the GBD of SEPT7 (Fig. 4A). However, the C-terminus (C′) of SEPT12 did not interact with that of SEPT7. In addition, SEPT12 also did not interact with the C′ of SEPT7 (Fig. 4B). These results indicate that SEPT12 and SEPT7 interact through their GBD domains, which is termed the G-interface.

We further assessed whether mutations within the G-interface (*SEPT12*^{D197N} and *SEPT12*^{T89M}) affected the SEPT12–SEPT7 association. The SEPT12^{T89M} mutation abolishes GTP hydrolytic activity, and the SEPT12^{D197N} mutation interferes with GTP binding (Kuo et al., 2012). The conservation of human SEPT12 T89 and D197 were evaluated in other septin subfamilies by multiple sequence alignment. T89 was conserved in the SEPT2, SEPT3 and SEPT7 subgroups, whereas D197 was conserved in all septin subgroups (supplementary material Fig. S3). To achieve the equal expression of wild-type SEPT12 (SEPT12^{WT}) and the mutants (SEPT12^{T89M} and SEPT12^{D197N}), we transfected different amounts of a SEPT12^{WT} plasmid. Transfection of 0.3 µg of the SEPT12^{WT} plasmid resulted in similar protein amounts to those obtained with the transfection of 1 µg of the SEPT12^{T89M} or 1 µg of the SEPT12^{D197N} plasmid in NT2/D1 cells (Fig. 4C). We co-expressed SEPT7 with SEPT12^{WT}, SEPT12^{T89M} or SEPT12^{D197N} in NT2/D1 cells. Wild-type SEPT12 but not the SEPT12 mutants could co-immunoprecipitate with SEPT7 (Fig. 4D). Thus, the mutations within the G-interface of SEPT12 disrupted the SEPT12–SEPT7 interaction. In addition, the subcellular localizations were also examined by immunostaining. The results obtained with SEPT12^{WT} showed that over 80% of the SEPT7 colocalized with SEPT12^{WT} in the NT2/D1 cells (Fig. 4E). However, the signals of the SEPT7 and SEPT12 mutants exhibited very little overlap in most cells analyzed. These data indicate that the G-interface of SEPT12 is crucial for the association of SEPT12 with SEPT7. In addition, wild-type

Journal of Cell Science (2015) 128, 923–934 doi:10.1242/jcs.158998

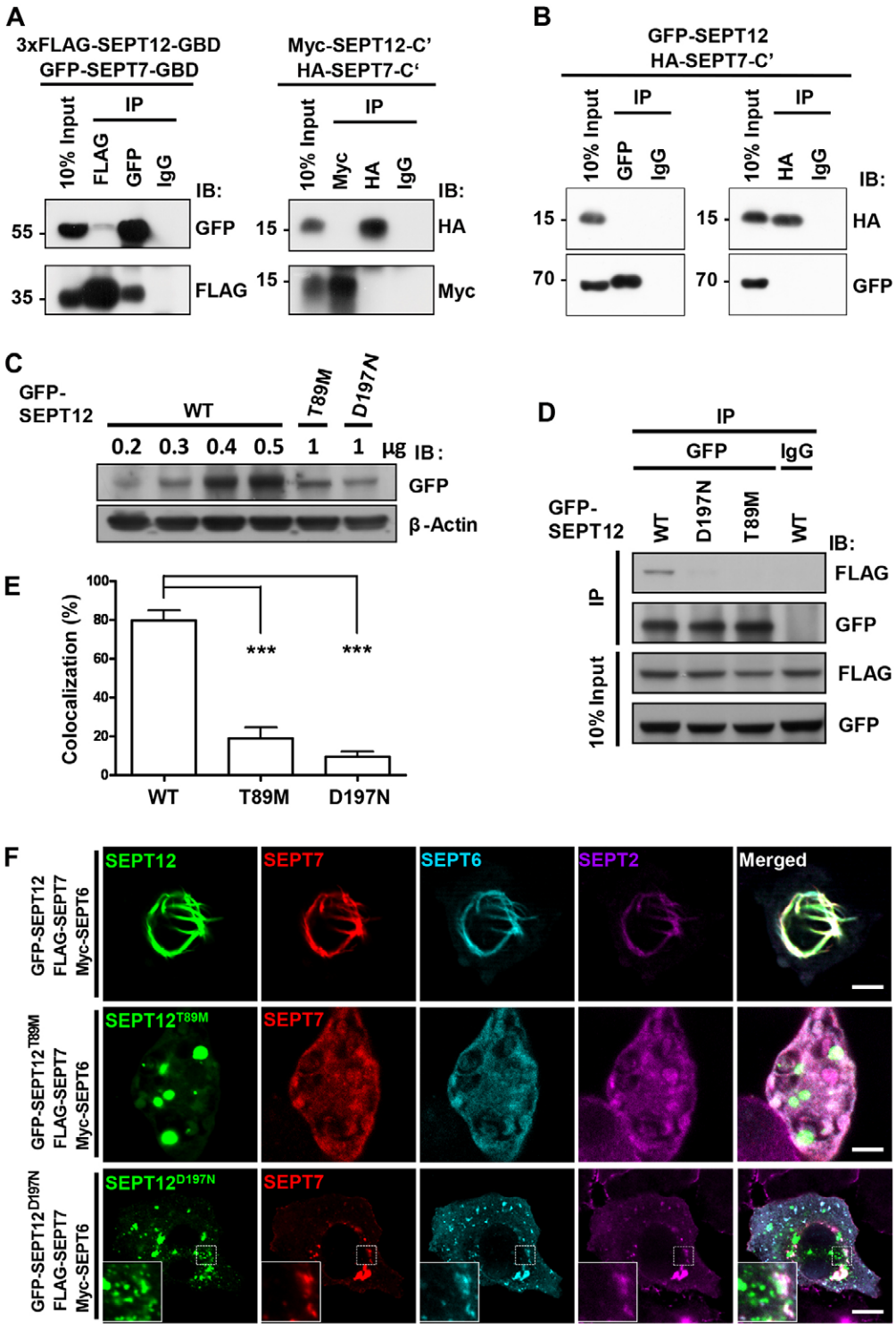

Fig. 4. See next page for legend.

SEPT12 formed filamentous structures with SEPT7, SEPT6, and SEPT2 in the NT2/D1 cells (Fig. 4F, top panel), whereas the SEPT12 mutants failed to form filamentous structures and did not colocalize with SEPT7, SEPT6 or SEPT2 (Fig. 4F, bottom panels). Interestingly, SEPT7, SEPT6 and SEPT2 still partially colocalized with each other in punctate particles (Fig. 4F, inset). These findings indicate that the mutations within the G-interface of SEPT12 dissociated SEPT12 from SEPT7–SEPT6–SEPT2 and disrupted SEPT12 filament formation.

To further confirm the interaction between SEPT12 and the SEPT7–SEPT6–SEPT2 complex, we co-expressed SEPT7, SEPT6 and SEPT2 with either the wild-type or mutant SEPT12 in 293T cells from a cell line devoid of endogenous SEPT12. Wild-type but not mutant SEPT12 interacted with SEPT7, SEPT6

Journal of Cell Science (2015) 128, 923–934 doi:10.1242/jcs.158998

Fig. 4. The SEPT12^{T89M} and SEPT12^{D197N} mutations in the GTP-binding domain cause SEPT12 to dissociate from the SEPT7–SEPT6–SEPT2 complex. (A,B) NT2D1 cells were co-transfected with various plasmids, as shown at the top. Lysates from transiently transfected cells were immunoprecipitated (IP) with the indicated antibodies, and IgG served as a negative control. Immunoblotting (IB) was carried out with the indicated antibodies shown on the right. Lanes showing 10% of the input are also present. Co-immunoprecipitation and reciprocal immunoprecipitation of FLAG–SEPT12-GBD with GFP–SEPT7-GBD, Myc–SEPT12-C′ with HA–SEPT7-C′ (A) and GFP–SEPT12 with HA–SEPT7-C′ (B). (C) Comparison of wild-type (WT) and mutant SEPT12 expression. NT2/D1 cells were transfected with different amounts of SEPT12^{WT} plasmid and mutants (SEPT12^{T89M} and SEPT12^{D197N}), as shown at the top. Immunoblotting was performed of the lysates with the indicated antibodies. (D) Co-immunoprecipitation of GFP–SEPT12^{WT}, GFP–SEPT12^{T89M} and GFP–SEPT12^{D197N} with FLAG–SEPT7. Immunoblotting was carried out with the indicated antibodies, as shown on the right. (E) SEPT7 does not colocalize with SEPT12 mutants in NT2D1 cells. Percentages of transfected cells showing colocalization of SEPT12 and SEPT7. FLAG–SEPT7 was co-transfected with EGFP–SEPT12^{WT}, EGFP–SEPT12^{T89M}, or EGFP–SEPT12^{D197N} into NT2/D1 cells. The distributions of the fusion proteins in the transfected cells were examined. The quantification bar was based on the observation of more than 100 cells. The data represent the mean±s.e.m. (n=3). ***P<0.001 (one-way ANOVA with Tukey's multiple comparison test for posterior comparisons). (F) SEPT12 colocalizes with SEPT7, SEPT6 and SEPT2 in a filament pattern, whereas SEPT12 mutants disrupt the filaments of all four septins. NT2D1 cells were co-transfected with various plasmids, as shown on the left. Representative images from the immunofluorescence staining showing the subcellular patterns of GFP–SEPT12, FLAG–SEPT7 and Myc–SEPT6, and endogenous SEPT2 in the cells transfected with wild-type SEPT12, SEPT12^{T89M} or SEPT12^{D197N}. The boxed areas, which are magnified in the insets, show the dissociation of SEPT12 from SEPT7, SEPT6 and SEPT2 in punctate patterns. Scale bars: 5 µm.

and SEPT2 (supplementary material Fig. S4). Taken together, these results show that the GTP binding and GTP hydrolytic activities of SEPT12 are required for the association of SEPT12 with the SEPT7–SEPT6–SEPT2 complex, resulting in SEPT12 filament formation.

SEPT12 filament is elongated by SEPT12-SEPT12 interaction through NC-interface

Considering that SEPT complexes join end-to-end to polymerize into filaments, it is likely that SEPT12, which holds a terminal position in the octamer, self-dimerizes through the NC-interface. To test this model, plasmids encoding differentially tagged full-length SEPT12 or its C-terminus were co-transfected into NT2/D1 cells. We found that SEPT12 interacted with itself because GFP–SEPT12 was co-immunoprecipitated with FLAG–SEPT12 (Fig. 5A). Moreover, Myc–SEPT12-C′ interacted with FLAG–SEPT12-C′ (Fig. 5B). These data indicate that SEPT12 interacts with itself through the C-terminus. Because a high salt concentration abolishes septin complex polymerization (Sellin et al., 2011), we performed immunoprecipitation under high-salt conditions to prove that SEPT12 filaments are elongated through the SEPT12 C-terminus. Plasmids encoding the differentially tagged C-terminus of SEPT12 were co-transfected into NT2/D1 cells. FLAG–SEPT12-C′ interacted with the HA–SEPT12-C′ under the low-salt conditions of immunoprecipitation (Fig. 5C, line 3). However, this interaction was dramatically reduced by high salt concentrations (Fig. 5C, line 2). These findings suggest that the SEPT12 C-terminus is responsible for septin complex polymerization.

We further investigated whether the SEPT12 NC-interface is required for polymerization of the SEPT 12-7-6-2 complex into filaments. SEPT12-GBD, which lacks both the N- and C-termini of SEPT12, was expressed in NT2/D1 cells to examine whether this mutant could disrupt filament formation. The SEPT12-GBD associated with SEPT7, SEPT6 and endogenous SEPT2, suggesting that the SEPT12-GBD still interacted with SEPT7, SEPT6 and SEPT2 as the core complex (Fig. 5D). However, the SEPT12-GBD disrupted the filament formation for all four septins (Fig. 5E). These findings indicate that the SEPT12 mutant lacking N- and C-termini formed a complex with SEPT7, SEPT6 and SEPT2 but failed to polymerize into filaments. Thus, the NC-interface of SEPT12 is dispensable for interactions within core complexes but is required for the polymerization of the complexes into filaments. Taken together, these results suggest that the SEPT 12-7-6-2 complexes are elongated into filaments through the SEPT12 NC-interface.

The SEPT12 filament is crucial for the structural integrity and motility of the sperm tail

To explore the manner by which the SEPT12 filament controls sperm functions, we studied the expression patterns of SEPT12, SEPT7, SEPT6, SEPT2 and SEPT4 in an infertile man carrying the SEPT12^{D197N} mutation. In the fertile control, immunofluorescence staining of the sperm showed strong SEPT12, SEPT7, SEPT6, SEPT2 and SEPT4 signals at the sperm annulus (Fig. 6A–D). However, all five septins were absent from the sperm annulus in the SEPT12^{D197N} patient, in whom the sperm had a defective annulus and bent tail (Fig. 6E–H). These data suggest that defective GTP binding of SEPT12, which perturbs the formation of the SEPT12-7-6-2 and 12-7-6-4 filaments, disrupts the SEPT ring structure of the sperm annulus and results in a defective sperm tail.

To further address the role of the SEPT12 filament in sperm maturation, we generated SEPT12 mutant mice carrying a SEPT12^{D197N} mutation. The testis sizes of SEPT12 heterozygous and homozygous mutant males were normal compared with wild-type males, as shown by the ratio of the organ weight the body weight (Fig. 7A, top panel). There was no significant difference in the number of spermatozoa isolated from the vas deferens. These data suggest that the SEPT12 mutant males had mature reproductive organs and normal mitotic and meiotic stages of sperm proliferation. However, sperm motility was reduced in the SEPT12 heterozygous mutant mice compared with the wild-type mice, and the SEPT12 homozygous mutant mice had more severe phenotypic alterations. These results demonstrate that the SEPT12 filament is required for sperm motility in a dose-dependent manner.

Next, we performed a morphological analysis of SEPT12 mutant sperm (Fig. 7A, middle and bottom panel). SEPT12 heterozygous mutant mice showed no obvious morphological sperm defects in the head, annulus or tail structures. However, the sperm of the SEPT12 homozygous mutant mice were rarely normal, presenting with either a defective annulus or a bent tail. Evaluation of the expression patterns of SEPT12, 7, 6 and 2 in these mice indicated that the levels of SEPT12, SEPT7, SEPT6 and SEPT2 were slightly decreased at the sperm annulus in the SEPT12$^{+/D197N}$ mice compared with the wild-type mice, and all four septins were absent in the SEPT12$^{D197N/D197N}$ mice (Fig. 7B). These results suggest that the sperm tail of the SEPT12 heterozygous mice might still maintain a normal appearance, but that the SEPT ring structure of the sperm annulus might be partially disrupted or the septin filaments at the sperm annulus might become unstable. In addition, the SEPT12 homozygous mice showed a disruption of the SEPT ring structure

Journal of Cell Science (2015) 128, 923–934 doi:10.1242/jcs.158998

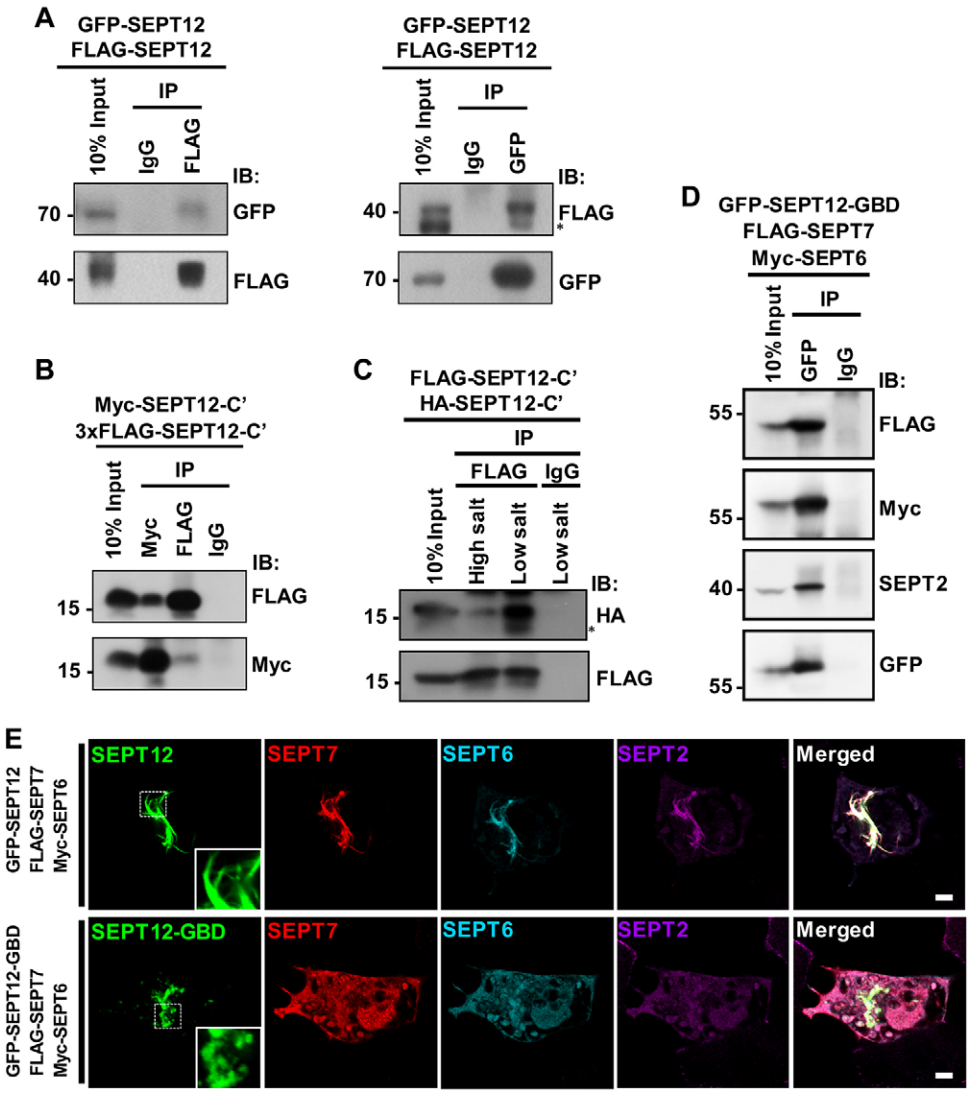

Fig. 5. The NC-terminus of SEPT12 is required for SEPT12-complex polymerization. (A–D) NT2D1 cells were co-transfected with various plasmids, as shown on the top. Lysates from transiently transfected cells were immunoprecipitated (IP) with the indicated antibodies, and IgG served as a negative control. Immunoblotting (IB) was carried out with the indicated antibodies, as shown on the right. Lanes showing 10% of the input are also present. The asterisk represents a nonspecific band. (A,B) Co-immunoprecipitation and reciprocal immunoprecipitation of FLAG–SEPT12 with GFP–SEPT12 (A) as well as Myc–SEPT12-C′ with FLAG–SEPT12-C′ (B). (C) Co-immunoprecipitation of FLAG–SEPT12-C′ with HA–SEPT12-C′ in 150 mM NaCl (low salt concentration) or 500 mM NaCl (high salt concentration). (D) Co-immunoprecipitation of GFP–SEPT12-GBD with FLAG–SEPT7, Myc–SEPT6 and endogenous SEPT2. (E) SEPT12-GBD lacking the N- and C-termini disrupts SEPT12, SEPT7, SEPT6 and endogenous SEPT2 filaments. NT2D1 cells were co-transfected with various plasmids, as shown on the left. Representative images from the immunofluorescence staining showing the subcellular patterns of GFP–SEPT12, FLAG–SEPT7, Myc–SEPT6 and endogenous SEPT2 in the cells transfected with full-length SEPT12 or its GTP-binding domain. The insets, which are magnified images, show filaments of wild-type SEPT12 or puncta of mutant SEPT12. Scale bars: 5 µm.

in the sperm annulus, resulting in sperm with a defective annulus and bent tail. Thus, SEPT12 filament formation is dispensable for the maturation of reproductive organs and sperm proliferation but is crucial for the structural integrity and motility of the sperm tail during postmeiotic differentiation of spermatogenesis.

DISCUSSION

In this study, we revealed the assembly order of the SEPT12-containing octamer complex, which is important for mammalian spermiogenesis (Fig. 8). SEPT12 filaments consisted of core complexes composed of the SEPT proteins 12-7-6-2-2-6-7-12, and SEPT4, which belongs to the same subgroup as SEPT2, could also occupy the same position as SEPT2 in the complex. SEPT12 interacted with SEPT7 through the GTP-binding domain (G-interface) and interacted with itself through the NC-terminus (NC-interface) to polymerize octamers into filaments. Two mutations within the GBD of SEPT12 (SEPT12^{D197N} and SEPT12^{T89M}) resulted in its dissociation from the SEPT7–SEPT6–SEPT2 complex, perturbing SEPT12 filament formation. An infertile patient carrying an SEPT12^{D197N} mutation has an absence of SEPT12, SEPT7, SEPT6, SEPT2 and SEPT4 signals at the annulus due to disrupted SEPT12 filament formation, resulting in a defective sperm annulus with a bent tail. In addition, analysis of SEPT12$^{D197N/D197N}$ mutant mice showed mature reproductive organs and a normal sperm count, but their sperm had a disorganized annulus, bent tail and reduced motility. These results indicate that the SEPT12 filament is specifically necessary for the terminal differentiation of germ cells. In conclusion, these findings illustrate that the SEPT12 octametric filament has an essential role of in the establishment of the annulus and sperm mechanical intensity during spermiogenesis.

Previous studies have shown that the human SEPT7–SEPT6–SEPT2 filament contains bound guanine nucleotides that are required for septin dimerization through the G-interface. Both SEPT2 and SEPT7 are GDP bound, and SEPT6 is GTP bound (Sirajuddin et al., 2007). It has been shown that SEPT12^{T89M} and SEPT12^{D197N} mutants lose their GTP hydrolytic and binding activities, respectively (Kuo et al., 2012). In this study, we further demonstrated that these mutants did not interact or colocalize with SEPT7 (Fig. 4), suggesting that human SEPT12 is GDP bound, similar to rat SEPT12 (Steels et al., 2007). We reasoned that SEPT12–SEPT7 dimerization was stabilized by the GDP–GDP interface in the SEPT 12-7-6-2 or 12-7-6-4 model. To date, only the filament comprising the SEPT proteins 7-6-2-2-6-7 has been characterized by crystallographic analysis. Kim et al. have

Journal of Cell Science (2015) 128, 923–934 doi:10.1242/jcs.158998

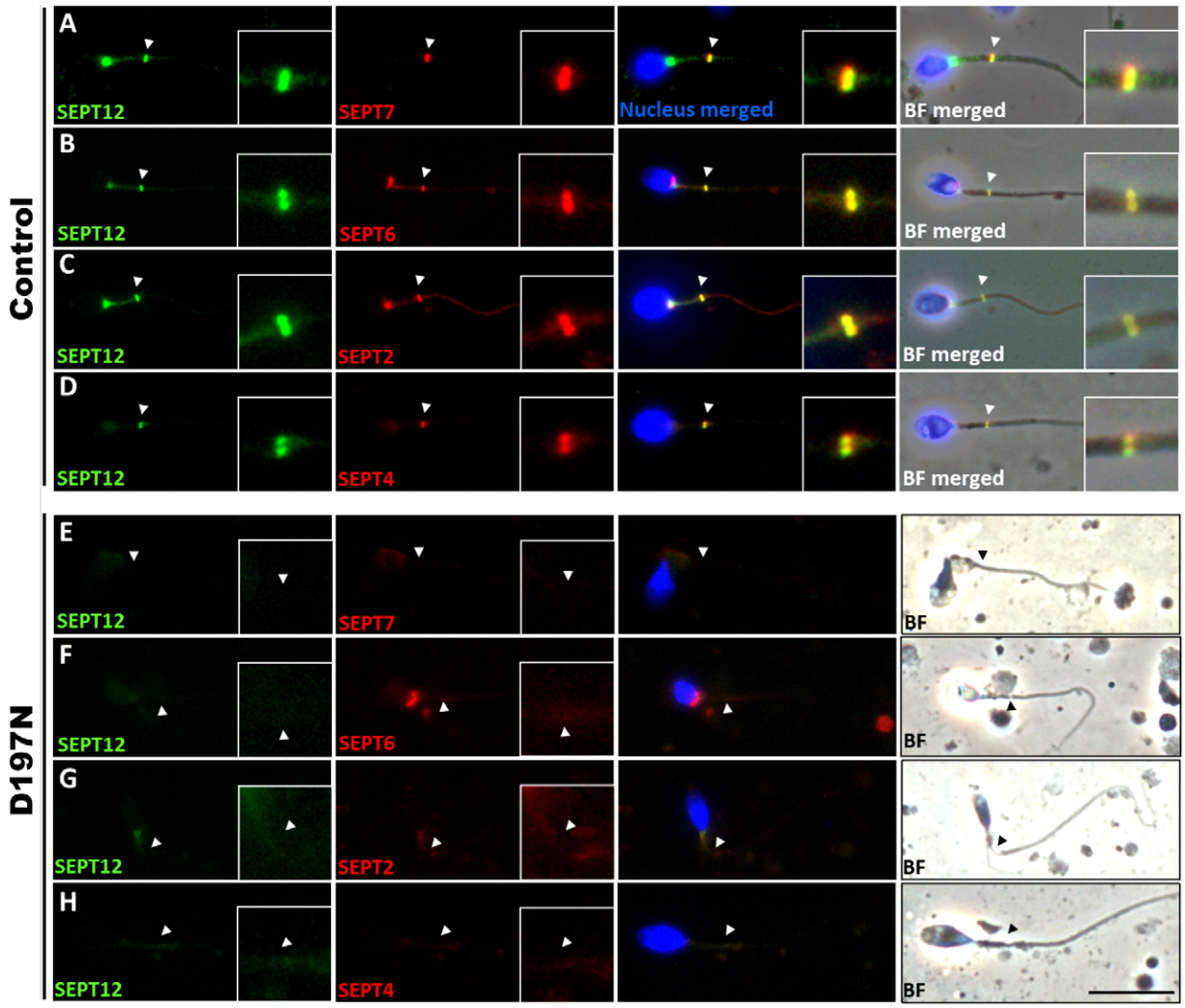

Fig. 6. Losses of SEPT12, SEPT7, SEPT6, SEPT2 and SEPT4 from the sperm annulus of a SEPT12^{D197N} patient. (A–D) Immunofluorescence staining of normal sperm in a fertile control showed signals for SEPT12 (A–D, green), SEPT7, SEPT6, SEPT2 and SEPT4 (A–D, red) at the annulus. Also shown are merged fluorescence staining images with the additional staining of the sperm nuclei, as well as merged fluorescence staining images with merged brightfield images (BF merged). (E–H) In the SEPT12^{D197N} patient, SEPT12, SEPT7, SEPT6, SEPT2 and SEPT4 staining produced no signals at the annulus of the abnormal sperm. Inset, magnified image of the annulus, as denoted by the arrowheads. Blue color, DAPI stain; BF, brightfield only. Scale bar: 10 μm.

implicated an octameric complex comprising the SEPT proteins 9-7-6-2-2-6-7-9 in midbody abscission during cytokinesis (Kim et al., 2011). Both SEPT12 and SEPT9 belong to the SEPT3 subgroup of the septin family, which lacks the C-terminal coiled-coil domain (Mostowy and Cossart, 2012). Our findings further strengthen the hypothesis that the assembly order of septin octamers is subgroup3-subgroup7-subgroup6-subgroup2-subgroup2-subgroup6-subgroup7-subgroup3. Although both SEPT9 and SEPT12 flank SEPT7–SEPT6–SEPT2 hexamers to form filaments, the roles of SEPT9- and SEPT12-depleted hexamers are different. In HeLa cells lacking SEPT9 expression, SEPT7–SEPT6–SEPT2 hexamers have been shown to adopt a suboptimal configuration, forming rudimentary filaments and smaller rings (Kim et al., 2011). However, an infertile man and mutant mice carrying the SEPT12^{D197N} mutation, which resulted in the dissociation of SEPT12 from the SEPT7–SEPT6–SEPT2 complex, showed the absence of all four septins from the sperm annulus and sperm with a defective annulus and bent tail (Figs 6 and 7). These findings imply that dissociation of SEPT12 from the SEPT7–SEPT6–SEPT2 hexamers disrupts their proper function and leads to the disappearance of these septins from the sperm annulus. Taken together, these results suggest that there is a function- or cell-specific regulation of the SEPT9- and SEPT12-associated SEPT7–SEPT6–SEPT2 hexamer.

The annulus is a septin-based fibrous ring structure connecting the midpiece and the principal piece of the mammalian sperm flagellum (Toure et al., 2011). The absence of an annulus is implicated in flagellum differentiation defects and human asthenozoospermia (poor sperm motility) (Lhuillier et al., 2009). Previous studies have demonstrated the presence of SEPT1, SEPT4, SEPT6 and SEPT7 in the sperm annulus (Ihara et al., 2005; Kissel et al., 2005). Infertile men carrying either SEPT12^{D197N} or SEPT12^{T89M} have been demonstrated to have various sperm defects involving the disorganization of the annulus and asthenozoospermia (Kuo et al., 2012). In addition, *Sept4*-null mice are sterile and have sperm with a defective annulus, bent tail and reduced motility, similar to an infertile man carrying SEPT12^{D197N} (Ihara et al., 2005; Kissel et al., 2005).

Journal of Cell Science (2015) 128, 923–934 doi:10.1242/jcs.158998

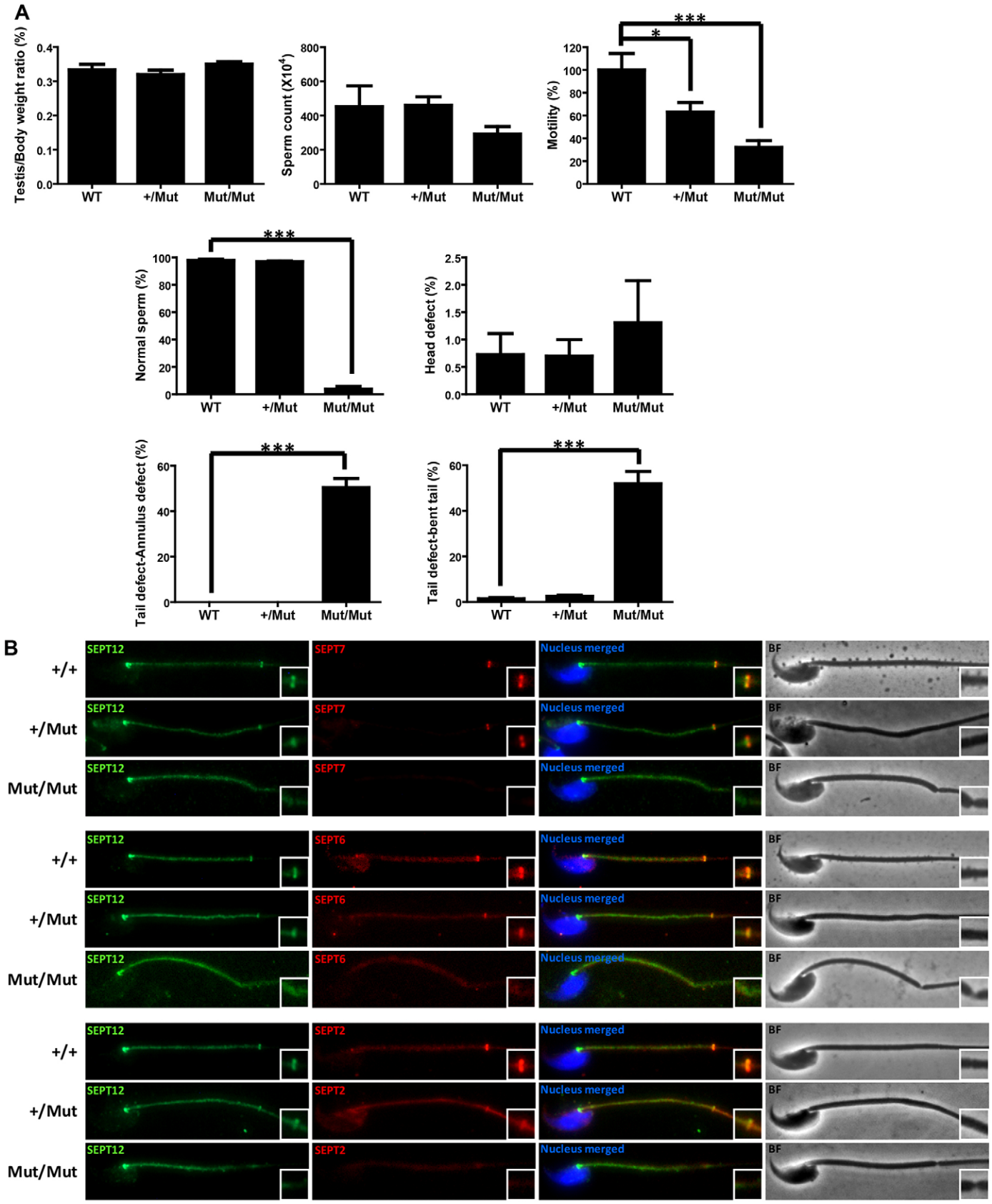

Fig. 7. See next page for legend.

Journal of Cell Science (2015) 128, 923–934 doi:10.1242/jcs.158998

Fig. 7. Sperm of SEPT12$^{D197N/D197N}$ mutant mice show reduced motility, a disorganized annulus, bent tails and absence of SEPT12, SEPT7, SEPT6 and SEPT2 signals. (A) Quantitative representation of testis:body weight ratio, sperm count ($\times10^4$), sperm motility and sperm morphological analysis in wild-type (WT), SEPT12$^{D197N/+}$ (+/Mut) and SEPT12$^{D197N/D197N}$ (Mut/Mut) mutant sperm. Sperm were isolated from the vas deferens. The data represent the mean±s.e.m. (WT, n=6; SEPT12$^{D197N/+}$, n=22; SEPT12$^{D197N/D197N}$, n=22). *P<0.05, **P<0.01, ***P<0.001 (Student's t-test). (B) Immunofluorescence staining of SEPT12, SEPT7, SEPT6 and SEPT2 at the annulus in wild-type, SEPT12$^{D197N/+}$ and SEPT12$^{D197N/D197N}$ mutant sperm. Also shown are merged fluorescence staining images with additional staining of the sperm nuclei, as well as brightfield images (BF). Inset, magnified image of the sperm annulus. Blue color, DAPI stain; BF, brightfield only.

Although several studies have demonstrated the presence of septins in the sperm annulus, the organization of the septin ring structure remains unclear. Here, we identified the octameric filaments composed of the SEPT proteins 12-7-6-2-2-6-7-12 and 12-7-6-4-4-6-7-12 as structural components of the annulus, and that defective SEPT12 filament formation disrupted the SEPT ring structure and annulus, and motility of the sperm tail. Thus, the SEPT12 octameric filament is indispensable for the structural and mechanical integrity of sperm. In this study, we also found that SEPT4 and SEPT2 were in the same septin family subgroup and could hold the same position in the SEPT12 core complex. We speculated that other septins, such as SEPT1, which is a member of SEPT6 subgroup, could occupy the same position as

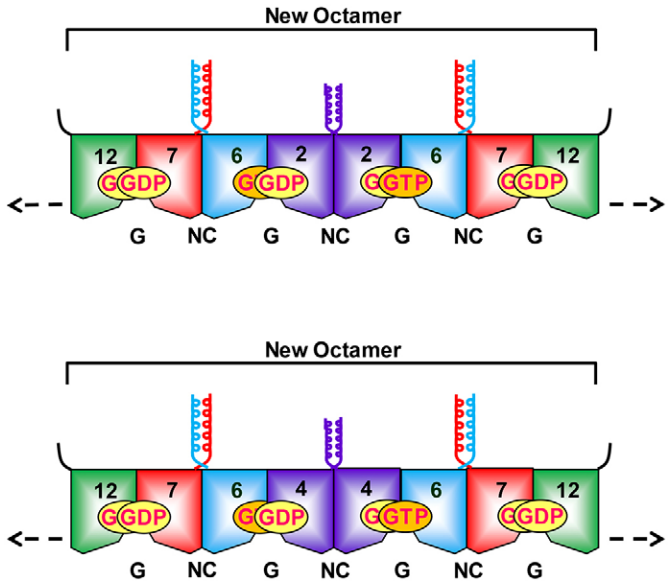

Fig. 8. Working models for formation of SEPT12 filament fibers in sperm annulus. SEPT12 associates with SEPT7, SEPT6 and SEPT2 or SEPT4 to form the SEPT 12-7-6-2-2-6-7-12 and 12-7-6-4-4-6-7-12 filaments. SEPT12 interacts with SEPT7 through the GTP-binding domain (G-interface) and elongates the filament with the addition of the SEPT12 octamer through a self-interaction through the NC-terminus (NC-interface). The loss of the GTP binding (SEPT12^{D197N}) and GTP hydrolytic activities (SEPT12^{T89M}) of SEPT12 result in the dissociation of SEPT12 from the SEPT7–SEPT6–SEPT2 complex. Human and mouse SEPT12^{D197N} sperm showed a defective annulus and reduced motility, indicating that SEPT 12-7-6-2-2-6-7-12 and 12-7-6-4-4-6-7-12 filament formation is important for the establishment of the annulus and sperm motility. The dotted arrows indicate the elongation of the filament with the addition of the SEPT octamers. NC, the N- and C-termini of the septin proteins (NC-interface). G, the GTP-binding domain of septins (G-interface).

SEPT6 in the SEPT12 complex. Future investigations will determine whether other septins are involved in the SEPT12 filament or form additional septin filaments that coordinate with these filaments to organize into the exact architecture of the annulus.

SEPT12$^{+/D197N}$ heterozygous mice displayed less severe deficiency compared with the infertile man carrying the SEPT12^{D197N} mutation (Figs 6 and 7). There are several differences in spermatogenesis between humans and mice, including species-specific numbers of spermatogenic stages, sperm morphology and spermatogenic efficiency (Hess and Renato de Franca, 2008; Borg et al., 2010). For example, the total duration of spermatogenesis is very long in humans compared with most mammals. In humans, the entire spermatogenic process lasts 70 days. However, it only lasts ~39–40 days in mice. By contrast, there are enormous variations in lifespan and reproductive span between the two species. Humans have a lifespan of ~70 years and a reproductive span of ~40 years. However, the lifespan and reproductive span of mice are only ~1.5–2 years and 1–2 years, respectively (Demetrius, 2005). Therefore, the cumulative effects of mutant proteins might be different between the two species. Comparative analysis of human and mouse genomes has revealed that many mouse-specific gene clusters are related to reproduction (Waterston et al., 2002). Most mouse-specific clusters correspond to a single gene in the human genome. The 'reproduction' clusters contain genes that have roles in spermatogenesis, such as survival and the fertilizing efficacy of spermatozoa. These factors might account for the different sensitivities of sperm to mutations between humans and mice.

In conclusion, these findings provide new insights into the detailed organization of the sperm annulus. In addition, our findings reveal new pathways of spermatogenesis and a new cause of reproductive failure. Considering that SEPT12 is specifically expressed in germ cells and functions in terminal differentiation during spermiogenesis, it represents an ideal target for a reversible male contraceptive that would not interfere with hormone function and would lead to minimal side effects.

MATERIALS AND METHODS

Clinical information

The study was approved by the Institutional Review Board of the National Cheng Kung University Hospital and Kuo General Hospital, Taiwan and all clinical samples were obtained with informed consent of all participants. From January 2005 to July 2007, infertile men with abnormal semen parameters, as well as fertile men with normal semen parameters, were enrolled. The detailed clinical information and genotypes of the patients have been described previously (Kuo et al., 2012). The patient and control subjects were Han Taiwanese, which is the major ethnic group in Taiwan (comprising more than 95% of the population).

DNA constructs, cell culture and transfection

Full-length complementary DNAs (cDNAs) of wild-type *SEPT2* (GenBank NP_001008491.1), *SEPT6* (GenBank NM_145799.3), *SEPT7* (GenBank BC093642.1) and *SEPT12* (GenBank NM_144605.4) were generated by PCR amplification of human testis cDNA (Human Total RNA Master Panel II; Clontech, Mountain View, CA). The sequences of these genes were retrieved from the NCBI database (http://www.ncbi.nlm.nih.gov/). *SEPT7* and *SEPT12* were cloned into the *Hin*dIII/*Bam*HI and the *Hin*dIII/*Xba*I sites, respectively, of pFLAG-CMV-2 (Sigma-Aldrich, St. Louis, MO). *SEPT12* was also cloned into the *Nhe*I/*Eco*RI sites of pEGFP-N1 (Clontech). *SEPT2* and *SEPT4* were cloned into the *Eco*RI/*Eco*RVsites and *Bam*HI/*Xho*I sites of pCDNA3-HA (Invitrogen), respectively. *SEPT6* was cloned into pCDNA3.1/myc-His (Invitrogen) at

the *Kpn*I/*Not*I sites. Mutant constructs (pEGFP-SEPT12^{T89M} and pEGFP-SEPT12^{D197N}) were generated with the original pEGFP-SEPT12WT plasmids using a QuikChange II site-directed mutagenesis kit (Stratagene, La Jolla, CA) according to the manufacturer's instructions. For the production of truncated septin proteins, DNA segments encoding the GTP-binding domains of SEPT12 and SEPT7 (amino acids 46–319 and 28–298, respectively) were generated by PCR and cloned separately into p3xFLAG-myc-CMV-26 (Sigma-Aldrich) and pEGFP-C3 (Clontech) at the *Hin*dIII/*Kpn*I sites. A DNA segment encoding the C-terminal portion of SEPT12 (amino acids 258–358) was generated and cloned separately into the *Eco*RI/*Xba*I sites of p3xFLAG-CMV-14 (Sigma-Aldrich), the *Eco*RI/XhoI sites of pCDNA3.1/myc-His (Invitrogen) and the *Eco*RI/*Xho*I sites of pCDNA3-HA (Invitrogen). Another DNA segment encoding the C-terminus of SEPT7 (amino acids 299–418) was also generated and cloned into the *Eco*RI/*Xho*I sites of pCDNA3-HA (Invitrogen). All constructs were verified by DNA sequencing analysis. For transient transfection, malignant human testis pluripotent embryonic carcinoma NT2/D1 cells were maintained in Dulbecco's minimal essential medium (DMEM) supplemented with 10% fetal bovine serum (FBS) and 1% antibiotics. The NT2/D1 cells were transfected using Lipofectamine 2000 (Invitrogen, Carlsbad, CA) according to the manufacturer's instructions. After 48 h, the cells were harvested for immunofluorescence staining and immunoblotting.

Immunoprecipitation assay, western blot analysis and immunofluorescence staining

Lysates from transiently transfected NT2/D1 cells were immunoprecipitated with anti-GFP (Abcam, Cambridge, UK), anti-FLAG (Sigma-Aldrich, St. Louis, MO), anti-Myc (Abcam, Cambridge, UK) or anti-HA (Covance, Princeton, NJ) antibodies at 4℃ for 6 h on a rotator, followed by incubation with Protein-G–Sepharose (GE Healthcare, Buckinghamshire, UK) at 4℃ overnight. Beads were collected by a brief centrifugation and washed three times with PBS buffer. The precipitates were resuspended in SDS sample buffer and denatured at 95℃ for 5 min. For western blotting, proteins were separated by SDS-PAGE and blotted onto nitrocellulose membranes. The blots were incubated with anti-GFP (1:2000, Santa Cruz Biotechnology, Inc., Santa Cruz, CA), anti-FLAG (1:2000), anti-Myc (1:3000) or anti-HA (1:5000) antibody. For immunofluorescence staining, human spermatozoa were stained with an anti-SEPT12 (1:100; Abnova, Taipei, Taiwan), anti-SEPT7 (1:50; Santa Cruz Biotechnology), anti-SEPT6 (1:100; Santa Cruz Biotechnology) or anti-SEPT2 antibody (1:200; Proteintech, Chicago, IL, USA) or MitoTracker Red 580 (Molecular Probes, Eugene, OR, USA) according to published procedures (Lin et al., 2009). The transfected NT2/D1 cells were fixed with 4% paraformadehyde in PBS, permeabilized with methanol, and blocked with antibody diluent (Dako, Glostrup, Denmark). The cells were incubated with an anti-GFP (1:800; Abcam), anti-FLAG (1:200), anti-Myc (1:400) or anti-SEPT12 (1:100) antibody at room temperature for 1 h and washed with TBST (0.02% Tween 20 in Tris-buffered saline) three times, followed by Alexa-Fluor-350-, Alexa-Fluor-488-, Alexa-Fluor-568- or Alexa-Fluor-660-labeled secondary antibody staining (1:200; Molecular Probes, Eugene, OR, USA) and a wash with 0.02% TBST. The nuclei were counterstained with 4,6-diamidino-2-phenylindole (DAPI). The cells were then visualized with an upright fluorescence microscope (Olympus, Tokyo, Japan) or a multiphoton laser scanning microscope (FV1000MPE, Olympus) under identical settings.

Generation of SEPT12^{D197N} mice

A genomic fragment carrying the entire mouse *Sept12* locus was constructed in a bMQ-374d12 BAC clone (Sanger Institute, Cambridge, UK). The genomic fragment of Septin12 constructed in pL253 was used to replace the wild-type allele of Septin12 in 129Sv mouse embryonic stem cells (ESCs). The missense mutation SEPT12 D197N (GAC to AAC) was introduced by PCR during the preparation of the targeting vector. The mutagenic primers used were 5′-AATGGTCAGGCTG-TTAGCCCGGGCGATCAC-3′ and 5′-GTGATCGCCCGGGCTAACA-GCCTGACCATT-3′. The entire sequence was verified by sequencing. The targeting vector was then transfected into 129Sv mouse embryonic stem cells by electroporation. ESC clones containing the targeted allele were selected and identified by Southern blot analysis. Several clones were isolated and transfected with a vector encoding Cre recombinase to excise the neo cassette and were then injected into C57BL/6J blastocysts. Chimeric males were bred with C57BL/6 females to produce heterozygous SEPT12D197N mice (F1). Homozygous SEPT12$^{D197N/D197N}$ mice (F2) were produced by mating SEPT12^{D197N} mice (F1) with each other. Wild-type and and SEPT12$^{D197N/D197N}$ littermates (F2) were bred, and tail genomic DNA was used for genotyping by PCR.

ClustalW multiple sequence alignment

Human septin family members were aligned using ClustalW2 program provided by EMBL-EBI (http://www.ebi.ac.uk/). The GenBank accession numbers for the SEPTIN proteins of *Homo sapiens* were as follows: SEPT1 (NP_443070.1), SEPT2 (NP_001008491.1), SEPT3 (isoform A, NP_663786.2; isoform B, NP_061979.3), SEPT4 (isoform 1, NP_004565.1; isoform 2, NP_536340.1; isoform 3, NP_536341.1), SEPT5 (NP_002679.2), SEPT6 (isoform A: NP_665798.1; isoform B: NP_055944.2; isoform D: NP_665801.1), SEPT7 (isoform 1, NP_001779.3; isoform 2, NP_001011553.2), SEPT8 (isoform A, NP_001092281.1; isoform B, NP_055961.1; isoform C, NP_001092282.1; isoform D, NP_001092283.1), SEPT9 (isoform A, NP_001106963.1; isoform B, NP_001106965.1; isoform C, NP_006631.2; isoform D, NP_001106967.1; isoform E, NP_001106964.1; isoform F, NP_001106968.1), SEPT10 (isoform 1, NP_653311.1; isoform 2, NP_848699.1), SEPT11 (NP_060713.1) and SEPT14 (NP_997249.2). The above information was obtained from the NCBI database (http://www.ncbi.nlm.nih.gov/).

Acknowledgements

We thank the technical services provided by the 'Transgenic Mouse Model Core Facility of the National Core Facility Program for Biotechnology, National Science Council' and the 'Gene Knockout Mouse Core Laboratory of National Taiwan University Center of Genomic Medicine'. We also thank Dr Pauline Yen (Institute Biomedical Sciences, Academia Sinica) for critical reading of the manuscript.

Competing interests

The authors declare no competing or financial interests.

Author contributions

Y.C.K., Y.R.S., C.Y.W. and P.L.K. developed the concept and designed experiments. Y.C.K., Y.R.S. and Y.Y.W. performed the experiments. Y.C.K., H.I.C., Y.H.L., Y.Y.W. and P.L.K. provided the acquisition of data (provided animals, acquired and managed patients, provided facilities, etc.). Y.C.K., Y.R.S., Y.R.C., C.Y.W. and P.L.K. analyzed the interpreted the data. Y.C.K., Y.R.S., C.Y.W. and P.L.K. wrote and reviewed the manuscript.

Funding

This study was supported by the from the National Science Council of the Republic of China [grant numbers NSC 96-2314-B-006-003; NSC 97-2628-B-006-012; NSC 98-2622-B-006-004; NSC 99-2628-B-006-027; NSC 100-2811-B006-043; andMOST 103-2314-B-006-036 to P.L.K.; and MOST 103-2314-B-006-037 to C.Y.W.].

Supplementary material

Supplementary material available online at
http://jcs.biologists.org/lookup/suppl/doi:10.1242/jcs.158998/-/DC1

References

Borg, C. L., Wolski, K. M., Gibbs, G. M. and O'Bryan, M. K. (2010). Phenotyping male infertility in the mouse: how to get the most out of a 'non-performer'. *Hum. Reprod. Update* **16**, 205-224.

Demetrius, L. (2005). Of mice and men. When it comes to studying ageing and the means to slow it down, mice are not just small humans. *EMBO Rep.* **6**, S39-S44.

Ding, X., Yu, W., Liu, M., Shen, S., Chen, F., Wan, B. and Yu, L. (2007). SEPT12 interacts with SEPT6 and this interaction alters the filament structure of SEPT6 in Hela cells. *J. Biochem. Mol. Biol.* **40**, 973-978.

Ding, X., Yu, W., Liu, M., Shen, S., Chen, F., Cao, L., Wan, B. and Yu, L. (2008). GTP binding is required for SEPT12 to form filaments and to interact with SEPT11. *Mol. Cells* **25**, 385-389.

Hess, R. A. and Renato de Franca, L. (2008). Spermatogenesis and cycle of the seminiferous epithelium. *Adv. Exp. Med. Biol.* **636**, 1-15.

Hong, S., Choi, I., Woo, J. M., Oh, J., Kim, T., Choi, E., Kim, T. W., Jung, Y. K., Kim, D. H., Sun, C. H. et al. (2005). Identification and integrative analysis of 28 novel genes specifically expressed and developmentally regulated in murine spermatogenic cells. *J. Biol. Chem.* **280**, 7685-7693.

Ihara, M., Kinoshita, A., Yamada, S., Tanaka, H., Tanigaki, A., Kitano, A., Goto, M., Okubo, K., Nishiyama, H., Ogawa, O. et al. (2005). Cortical organization by the septin cytoskeleton is essential for structural and mechanical integrity of mammalian spermatozoa. *Dev. Cell* **8**, 343-352.

Jarow, J. P., Sharlip, I. D., Belker, A. M., Lipshultz, L. I., Sigman, M., Thomas, A. J., Schlegel, P. N., Howards, S. S., Nehra, A., Damewood, M. D. et al.; Male Infertility Best Practice Policy Committee of the American Urological Association Inc. (2002). Best practice policies for male infertility. *J. Urol.* **167**, 2138-2144.

Kim, M. S., Froese, C. D., Estey, M. P. and Trimble, W. S. (2011). SEPT9 occupies the terminal positions in septin octamers and mediates polymerization-dependent functions in abscission. *J. Cell Biol.* **195**, 815-826.

Kinoshita, M. (2003). Assembly of mammalian septins. *J. Biochem.* **134**, 491-496.

Kissel, H., Georgescu, M. M., Larisch, S., Manova, K., Hunnicutt, G. R. and Steller, H. (2005). The Sept4 septin locus is required for sperm terminal differentiation in mice. *Dev. Cell* **8**, 353-364.

Kuo, Y. C., Lin, Y. H., Chen, H. I., Wang, Y. Y., Chiou, Y. W., Lin, H. H., Pan, H. A., Wu, C. M., Su, S. M., Hsu, C. C. et al. (2012). SEPT12 mutations cause male infertility with defective sperm annulus. *Hum. Mutat.* **33**, 710-719.

Lhuillier, P., Rode, B., Escalier, D., Lorès, P., Dirami, T., Bienvenu, T., Gacon, G., Dulioust, E. and Touré, A. (2009). Absence of annulus in human asthenozoospermia: case report. *Hum. Reprod.* **24**, 1296-1303.

Lin, Y. H., Lin, Y. M., Wang, Y. Y., Yu, I. S., Lin, Y. W., Wang, Y. H., Wu, C. M., Pan, H. A., Chao, S. C., Yen, P. H. et al. (2009). The expression level of septin12 is critical for spermiogenesis. *Am. J. Pathol.* **174**, 1857-1868.

Lin, Y. H., Wang, Y. Y., Chen, H. I., Kuo, Y. C., Chiou, Y. W., Lin, H. H., Wu, C. M., Hsu, C. C., Chiang, H. S. and Kuo, P. L. (2012). SEPTIN12 genetic variants confer susceptibility to teratozoospermia. *PLoS ONE* **7**, e34011.

Mostowy, S. and Cossart, P. (2012). Septins: the fourth component of the cytoskeleton. *Nat. Rev. Mol. Cell Biol.* **13**, 183-194.

Nagaraj, S., Rajendran, A., Jackson, C. E. and Longtine, M. S. (2008). Role of nucleotide binding in septin-septin interactions and septin localization in Saccharomyces cerevisiae. *Mol. Cell. Biol.* **28**, 5120-5137.

Sellin, M. E., Sandblad, L., Stenmark, S. and Gullberg, M. (2011). Deciphering the rules governing assembly order of mammalian septin complexes. *Mol. Biol. Cell* **22**, 3152-3164.

Sellin, M. E., Stenmark, S. and Gullberg, M. (2014). Cell type-specific expression of SEPT3-homology subgroup members controls the subunit number of heteromeric septin complexes. *Mol. Biol. Cell* **25**, 1594-1607.

Sirajuddin, M., Farkasovsky, M., Hauer, F., Kühlmann, D., Macara, I. G., Weyand, M., Stark, H. and Wittinghofer, A. (2007). Structural insight into filament formation by mammalian septins. *Nature* **449**, 311-315.

Sirajuddin, M., Farkasovsky, M., Zent, E. and Wittinghofer, A. (2009). GTP-induced conformational changes in septins and implications for function. *Proc. Natl. Acad. Sci. USA* **106**, 16592-16597.

Steels, J. D., Estey, M. P., Froese, C. D., Reynaud, D., Pace-Asciak, C. and Trimble, W. S. (2007). Sept12 is a component of the mammalian sperm tail annulus. *Cell Motil. Cytoskeleton* **64**, 794-807.

Toure, A., Rode, B., Hunnicutt, G. R., Escalier, D. and Gacon, G. (2011). Septins at the annulus of mammalian sperm. *Biol. Chem.* **392**, 799-803.

Versele, M. and Thorner, J. (2004). Septin collar formation in budding yeast requires GTP binding and direct phosphorylation by the PAK, Cla4. *J. Cell Biol.* **164**, 701-715.

Waterston, R. H., Lindblad-Toh, K., Birney, E., Rogers, J., Abril, J. F., Agarwal, P., Agarwala, R., Ainscough, R., Alexandersson, M., An, P. et al.; Mouse Genome Sequencing Consortium (2002). Initial sequencing and comparative analysis of the mouse genome. *Nature* **420**, 520-562.

Weirich, C. S., Erzberger, J. P. and Barral, Y. (2008). The septin family of GTPases: architecture and dynamics. *Nat. Rev. Mol. Cell Biol.* **9**, 478-489.

WHO (1999). *WHO Laboratory Manual for the Examination of Human Semen and Sperm–Cervical Mucus Interaction*. Cambridge: Cambridge University Press.